

WOOD ¹⁴C DATING WITH AIXMICADAS: METHODS AND APPLICATION TO TREE-RING SEQUENCES FROM THE YOUNGER DRYAS EVENT IN THE SOUTHERN FRENCH ALPS

Manuela Capano^{1*} • Cécile Miramont² • Frédéric Guibal² • Bernd Kromer³ • Thibaut Tuna¹ • Yoann Fagault¹ • Edouard Bard^{1*}

¹CEREGE, Aix-Marseille University, CNRS, IRD, Collège de France, Technopôle de l'Arbois, BP 80, F-13545 Aix-en-Provence, France.

²IMBE, Aix-Marseille University, CNRS, IRD, Avignon University, Technopôle de l'Arbois, 13545 Aix-en-Provence, France.

³Institute of Environmental Physics, University of Heidelberg, Germany.

ABSTRACT. The AixMICADAS facility is in part dedicated to research on radiocarbon (¹⁴C) calibration by means of various archives. For this purpose, we are improving upon the capacity to accurately date subfossil wood. In the current study, nine chemical pretreatment protocols are tested on six wood samples of known ages. The optimization based on ¹⁴C ages, ¹³C/¹²C ratios, carbon % and overall mass yield % leads us to favor the acid-base-acid-bleaching pretreatment (ABA-B). This efficient method is shown to provide a residue of holocellulose with optimal blanks equivalent to an age of 51,300 ¹⁴C BP with a standard deviation of 1500 yr based on 25 analyses. The seven wood samples from the Sixth International Radiocarbon Intercomparison (SIRI) are then analyzed as a further verification of the accuracy of our method. As a first scientific contribution, we studied two tree-ring sequences from subfossil pines (Barb12 and Barb17) collected in the southern French Alps. New ¹⁴C analyses were performed at high resolution (every third year) and are shown to agree well with results obtained previously by high precision β-counting on CO₂ from large samples at lower resolution for Barb17 and accelerator mass spectrometry (AMS) data for Barb12. The new ¹⁴C series are then matched to the Kauri and YDB chronologies: the new sequence of Barb12-17 tentatively corresponds to the interval between 12,836 and 12,594 cal BP within the Younger Dryas cold period. The ¹⁴C comparison between the Barb12-17 sequence from France and the Kauri sequence from New Zealand allows calculating the ¹⁴C Inter-Hemispheric Gradient (IHG), with an average value of ca. 57 yr. The IHG stayed relatively high throughout the studied period. Interestingly, the IHG exhibits a transient maximum value (ca. 100 yr) during the period of rapid Δ¹⁴C rise (12,750–12,720 cal BP), a behavior that could be due to a delayed response of the Southern Hemisphere.

KEYWORDS: ¹⁴C calibration, ABA, cellulose extraction, interhemispheric ¹⁴C gradient, SIRI 2013, subfossil wood, Younger Dryas event.

INTRODUCTION

One of the main projects linked to the installation of the AixMICADAS facility in Aix-en-Provence, France (Bard et al. 2015) is to contribute to radiocarbon (¹⁴C) calibration by means of various archives (Reimer et al. 2013). The most accurate and precise information comes from the dating of tree-ring sequences from subfossil wood. A necessary first step is to select and set up a suitable chemical pretreatment method for wood samples enabling their ¹⁴C dating by the accelerator mass spectrometry (AMS) facility of Aix-en-Provence.

Wood is mainly composed of cellulose (α-cellulose and hemicelluloses), lignin, and to a lesser extent, ash and extractives. The relative proportions of these different components depend on the wood species (Fengel and Wegener 1989). Ash represents inorganic material, while extractives are a mobile source of organic C translocated among rings (Tans et al. 1978; Harlow et al. 2006; Szymczak et al. 2011). There is consensus in the radiocarbon community that extractives need to be removed prior to ¹⁴C dating of tree rings. By contrast, the choice of which different wood structural fractions to isolate (bulk wood, holocellulose, or α-cellulose) is still under discussion (Southon and Magana 2010).

After reviewing a large body of literature on wood pretreatments, we carried out different techniques in order to optimize a protocol adapted to the main types of wood samples

*Corresponding authors. Email: capano@cerege.fr; bard@cerege.fr.

(i.e. modern and subfossil wood from coniferous and broadleaf trees). For this purpose, we performed numerous tests on known-age woods. Our criterion for the best pretreatment is the effectiveness of exogenous carbon removal—associated with short and simple procedures—which limits secondary contamination during sample pretreatment. The ^{14}C results are complemented with $\delta^{13}\text{C}$, C percentage and mass yield obtained from the different procedures.

We then used our selected method to date the wood samples of the Sixth International Radiocarbon Intercomparison (SIRI), in order to confirm the chosen method by comparing the results of our measurements with the consensus values obtained in the framework of the SIRI intercomparison. As a further validation and first scientific contribution, we analyzed important tree-ring sequences from subfossil pines collected in the southern French Alps. The new results at high resolution were then compared first with previous measurements obtained by high precision measurements on CO_2 from large samples (Kaiser et al. 2012) and then with ^{14}C results on Kauri trees from New Zealand (Hogg et al. 2016a, 2016b), enabling us to study the ^{14}C interhemispheric gradient during an interval of the Younger Dryas climatic event.

Previous Works on Wood Pretreatments

Several types of chemical pretreatment have been developed previously with differences aimed at targeting different wood ages (e.g. pre- or post-bomb; Stuiver and Quay 1981), different wood species (Hoper et al. 1998; Borella et al. 1998; Cullen and MacFarlane 2005; Rinne et al. 2005) or particular contaminants (Bruhn et al. 2001; Dee et al. 2011; Capano et al. 2012; Fedi et al. 2014).

The classical ABA (acid-base-acid) method described by de Vries and Barendsen (1954) is routinely used in many laboratories for the pretreatment of various organic samples, including wood. Largely modified in the different ^{14}C laboratories (Santos and Ormsby 2013), this method isolates the wood cellulose and lignin and removes exogenous inorganic and organic carbon. Nevertheless, the ABA treatment can leave behind a residual contamination in very old samples (i.e. blank ^{14}C samples; Santos et al. 2001; Southon and Magana 2010). For this reason, the isolation of the cellulose, the most stable wood component, could prove useful. Moreover, for studying post-bomb tree rings at annual resolution, it is extremely important to isolate the carbon assimilated in the corresponding growth year, as non-cellulosic compounds can be synthesized the year after the ring formation or can be translocated between several rings (Cain and Suess 1976; Gray and Thompson 1977; Leavitt and Danzer 1993; Anchukaitis et al. 2008).

An open question remains as to whether a particular cellulosic fraction (α -cellulose) should be extracted or if the isolation of the holocellulose (composed of α -cellulose and hemicelluloses) is sufficient. With the aim of isolating one of the most stable wood components, α -cellulose has been preferred, particularly in stable isotope analysis. Following the method proposed by Green (1963), several modifications have been developed to improve the protocol (Loader et al. 1997; MacFarlane et al. 1999; Rinne et al. 2005; Cullen and MacFarlane 2005; Gaudinski et al. 2005; Anchukaitis et al. 2008; Southon and Magana 2010; Staff et al. 2014).

Nevertheless, these α -cellulose extraction methods remain tedious and time consuming, and several studies have explored other procedures used in the chemical industry to obtain a residue similar to α -cellulose (Wallis et al. 1997; Macfarlane et al. 1999; Brendel et al. 2000; Cullen and MacFarlane 2005; Gaudinski et al. 2005; Anchukaitis et al. 2008; Nĕmec et al. 2010; Li and Liu 2013; Liu et al. 2015). Unfortunately, these industrial pretreatments may not be suitable for ^{14}C analyses (Gaudinski et al. 2005; Anchukaitis et al. 2008).

In addition, chemical analyses performed on isolated α -cellulose clearly show that some hemicellulose residues remain after the extraction (Green 1963; Loader et al. 1997; Wallis et al. 1997; Gaudinski et al. 2005). Fortunately, there does not seem to be a systematic difference between the ^{14}C results of α -cellulose and holocellulose residues (Southon and Magana 2010). The isolation of the holocellulose may thus be sufficient for ^{14}C analyses, above all because its separation is quicker than the full α -cellulose extraction.

I. TESTING WOOD PRETREATMENTS

MATERIAL AND METHODS

In order to choose the best treatment adapted to different conditions, several chemical protocols were performed on six samples of known age:

- a) IAEA-C3 is the cellulose standard, in which the certified F^{14}C is 1.2941 ± 0.0006 and the $\delta^{13}\text{C}$ is -24.9‰ (Rozanski et al. 1992).
- b) Quercus-1980 is the wood of an oak tree (*Quercus pubescens* Willd.) from Aix-en-Provence (France), which was cut in winter 2014–2015. Only the latewood of the ring corresponding to the year 1980 was sampled, in order to isolate the C assimilated in the corresponding growth year.
- c) Larix-1980 is the wood of a larch tree (*Larix decidua* Mill.) from the Alps of Haute Provence (France). The last ring before the bark is dated to 1994, and only the latewood of the ring corresponding to the year 1980 was isolated.
- d) COUT203 is the wood of a subfossil pine tree (*Pinus sylvestris* L.) from the Alps of Haute Provence (France). It has a sequence of 170 yr included in a floating chronology (Sivan et al. 2006; Miramont and Sivan 2008). The group of rings 150–160 from COUT203 tree, previously dated at the Poznan AMS laboratory to 7260 ± 40 BP after the ABA pretreatment, was analyzed.
- e) Plio is the wood of a fossil tree found in a canyon in Nice (France), corresponding to the Messinian period of the Pliocene (personal communication with Jean Claude Hippolyte). This sample is thus expected to be devoid of ^{14}C .
- f) VIRI-K is the wood of a Miocene tree, distributed as a blank in the framework of the Fifth International Radiocarbon Intercomparison (Scott et al. 2010).

The two modern wood samples (b, c) were chosen for the high precision dating comparison associated with the atmospheric ^{14}C bomb spike, assuming that the latewood grew between July and October 1980 (Hua et al. 2013). In addition, the chosen samples enable testing different species of trees, both broadleaf and coniferous, with greater difficulty expected for the delignification of the coniferous wood (Cullen and MacFarlane 2005). The two wood blanks were selected to quantify the modern carbon contamination. The state of preservation of Plio is not optimal as it shows charcoal consistency, probably due to advanced mineralization process, and it will thus be useful for selecting procedures able to pretreat fragile samples. Finally, COUT203 was chosen because it belongs to the same species and it comes from the same region as the subfossil wood used for our ^{14}C calibration project (Section II below).

Samples were sliced in small pieces (ca. 2 mm^3) and ca. 100 mg were isolated for most of them, with the exception of Plio, whose deteriorated wood required ca. 500 mg of material.

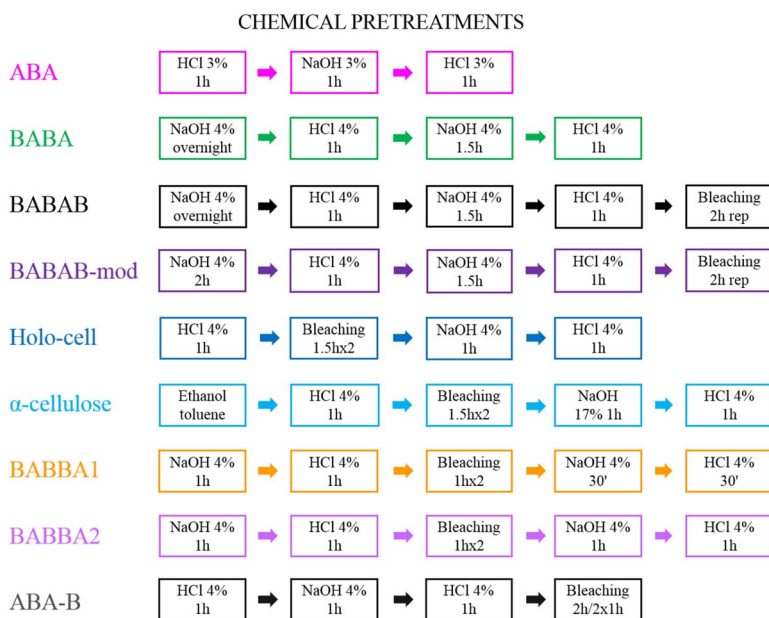


Figure 1 Schematic description of chemical pretreatments for dating wood; rep = repeatable step.

Based on previous experience (Capano et al. 2010, 2012, 2013) and review of the literature, we have used the following chemical protocols to process these samples. Figure 1 provides a visual summary of these procedures:

- ABA (acid-base-acid) method (de Vries and Barendsen 1954), with a modified procedure using HCl, NaOH, HCl at 3% concentration for 1 hr each (Passariello et al. 2007).
- BABA (base-acid-base-acid), an ABA method with 4% reagent solutions, preceded by an overnight bath in base solution (Kromer et al. 2010). It was performed for comparison with the standard ABA method, because high pH (i.e. first long alkaline bath) helps to dissociate the main wood components (Němec et al. 2010).
- BABAB (base-acid-base-acid-bleaching) method with solutions at 4% (Němec et al. 2010). This method entails an overnight alkaline bath for disrupting wood structure before the following treatment (Němec et al. 2010) and a bleaching step for holocellulose isolation.
- BABAB-mod is a BABAB modified method from Němec et al (2010). The difference with respect to the original pretreatment is the reduced duration for the initial bath in base solution to 2 hr, in order to reduce the overall duration of the process.
- Holo-cell is a more classical holocellulose extraction procedure modified from Capano et al. (2010). The treatment consists of the following: I) an HCl bath at 4% for 1 hr; II) bleaching (60 g of NaClO₂ in 1 L ultrapure H₂O in acid solution (HCl) at pH 3, repeated twice for 1.5 hr each); III) a NaOH bath at 4% for 1 hr, used to remove lignin residue and a portion of the hemicellulose residues (a step which is missing in the BABAB method); and IV) a final HCl bath at 4% concentration.
- α-cellulose extraction procedure modified from Cullen and MacFarlane (2005). In order to reduce procedural time, the soxhlet was substituted with several cycles of ultrasonic baths in

organic solvents: five 20-min baths in ethanol-toluene (1:2), five 20-min baths in ethanol, and five 20-min baths in ultrapure water. The following day, the cellulose extraction was performed as in the procedure described above [procedure e)], but with NaOH at 17%, which is the minimum concentration for the isolation of α -cellulose, according to Cross and Bevan (1912). This α -cellulose pretreatment lasts for two days and it is performed to test whether a better blank could be achieved.

- g) BABBA1 (base-acid-bleaching-base-acid) is the combining of the two holocellulose extraction methods (procedures d/ e/): the holo-cell treatment is preceded by a bath in NaOH, reduced to 1 hr. Bleaching is performed in two baths of 1 hr each; while the last NaOH and HCl baths are reduced to 30 min. The reaction time is reduced because the first alkaline bath should already disrupt wood structures and facilitate the cellulose extraction (Němec et al. 2010).
- h) BABBA2 (base-acid-bleaching-base-acid) is the same as BABBA1 (described above), but with 1-hr durations for the last NaOH and HCl baths.
- i) ABA-B is a classical ABA treatment followed by bleaching. Each bath in HCl, NaOH and HCl 4% solutions lasts for 1 hr. Bleaching was performed with 60 g of NaClO_2 in 1 L of ultrapure water in acid solution (HCl) at pH 3. The bleaching step was performed once for 2 hr and was repeated twice for 1 hr, in cases of difficult samples. This treatment omits the post-bleaching bath in base solution and, for this reason, it leads to a less purified holocellulose fraction than do previously tested methods [procedures e), g), h)].

All chemical treatments were performed in glass tubes on a heated block at 70°C, equipped with an agitation system. Solutions of at least 10 mL were changed using plastic pipettes and neutralized with ultrapure water. Finally, samples were oven dried overnight at 70°C.

Several studies extract the resins with a soxhlet apparatus also in holocellulose extraction procedures. However, some other studies omit this soxhlet step (e.g. Němec et al. 2010; Southon and Magana 2010) and Rinne et al. (2005) demonstrated that NaOH is sufficient to remove resins from *Pinus sylvestris*. Consequently, we also omitted the soxhlet step for the holocellulose extraction because our purpose is to select a simple and time-effective procedure.

Each chemical procedure was repeated at least three times on blank samples (Plio and VIRI-K), in order to quantify the reproducibility of blanks. Indeed, this is the parameter that matters most in the propagation of errors for unknown samples. In order to evaluate the ^{14}C contamination level before any pretreatments, all samples were additionally analyzed without pretreatment.

We measured the mass yield by weighing the initial dried sample and residue after pretreatment, as well as the C percentage by means of the elemental analyzer (EA, VarioMicroCube Elementar). The BABAB method was performed only to compare its mass yield with that of its modified version (BABAB-mod).

After chemical pretreatment, the dried residual samples were weighed in a tin capsule, combusted by using the EA, and the CO_2 was finally transformed into graphite with the AGE III system. The graphite target was then analyzed for its $^{14}\text{C}/^{12}\text{C}$ and $^{13}\text{C}/^{12}\text{C}$ ratios by means of AixMICADAS (Bard et al. 2015).

Standards (OxA2 NIST SRM4990C) and blanks (phthalic acid) were processed together with samples and used for normalization and blank correction. Blank samples (Plio and VIRI-K)

were not corrected for background. Two measurements for each chemical pretreatment were performed for all samples (three replicates for blanks).

An additional uncertainty of 1.6‰ was propagated in the ^{14}C analytical errors. This additional error is based on the long-term laboratory statistics of measurements of the IAEA-C3 standard, processed with the chosen chemical pretreatment (ABA-B). The ^{14}C data are reported in terms of conventional ^{14}C age BP and in terms of $F^{14}\text{C}$, which is the $^{14}\text{C}/^{12}\text{C}$ isotope ratio after normalization and blank correction (Stuiver and Polach 1977; Reimer et al. 2004; van der Plicht and Hogg 2006). The $^{13}\text{C}/^{12}\text{C}$ ratios are reported using the conventional δ notation by using OxA2 NIST standard. All reported values for C% and $^{13}\text{C}/^{12}\text{C}$ ratios are the average of at least two replicates and listed errors are the standard deviations (SD) among replicates.

Results on Mass Yield, C%, and $^{13}\text{C}/^{12}\text{C}$ Ratio

The mass yield after the different pretreatments varies extensively because it depends on the efficiency of the isolation of the wood fraction and the loss of unwanted material (Table 1). The wood mass yield probably also depends on the type of tree, its age and state of preservation. Additional sources of variability are found in the incidental physical loss of the sample at each liquid-solid separation performed by manual pipetting during the pretreatments. As suggested by three replications of blank samples this variability could be on the order of several percent (from 1 to 7%; Table 1).

As expected, the least aggressive procedure (ABA) leads to the highest mass recovery for the wood residue, whereas BABA leads to a more thorough extraction and, hence, to lower residual mass. For most samples, the α -cellulose extraction is the most aggressive pretreatment, leading to a smaller wood residue after extraction. In the case of the Plio blank wood, the sample disappeared completely in two α -cellulose extractions, while a very small residue amenable to ^{14}C dating was recovered in the third replicate. Because of this extremely poor incidence of recovery leading to sub-optimal ^{14}C results (see below), the α -cellulose treatment is clearly not optimal for our purposes.

An initial bath in base solution may already destroy part of the cellulose, as suggested by the results obtained on the C3 standard made of pure cellulose. Indeed, the mass yield for C3 is lower for the pretreatment procedures, which incorporate this initial step (BABAB-mod and BABBA1), than for those which omit it (Holo-cell and ABA-B).

In general, the ABA-B procedure is among the most thorough protocols leading to rather small residues for the various samples (Table 1). At the same time, this relatively simple method

Table 1 The yield mass (%) of all samples is given after each pretreatment method. Plio and VIRI_K values are followed by the standard deviation of replications of the same pretreatment.

	ABA	BABA	BABAB	BABAB-mod	Holo-cell	α -cellulose	BABBA1	BABBA2	ABA-B
C3	80	59	—	65	78	18	63	—	70
Quercus_1980	55	44	—	36	30	12	20	—	—
Larix_1980	63	54	16	35	24	11	25	20	29
COUT203	77	64	43	44	26	—	31	34	42
Plio	40 \pm 7	32 \pm 4	2	2 \pm 1	1 \pm 1	0.3 \pm 1	5 \pm 1	4 \pm 3	15 \pm 5
VIRI_K	72 \pm 5	62 \pm 4	12	24 \pm 6	6 \pm 6	15 \pm 2	20 \pm 1	18 \pm 3	29 \pm 1

allows preservation of a significant mass of the old and damaged Plio blank wood, enabling its subsequent ^{14}C dating (see below).

When the BABAB method is compared with its modified version (BABAB-mod), two samples (COUT203 and Plio) show the same % yield, while Larix-1980 and VIRI-K exhibit higher yields after the BABAB-mod. Although still compatible with random scatter, this may indicate that for well-preserved wood, the length of the initial bath in base solution results in the removal of more material as reaction time increases. By contrast, the BABBA1 and BABBA2 procedures lead to similar mass yields (Table 3), indicating that lengthening the final baths in basic and acidic solutions does not improve the extraction.

The molecular percentage of carbon in cellulose is 44.4% (Vertregt and de Vries 1987), but it frequently ranges from 43 to 45% (Cullen and MacFarlane 2005). This is compatible with the value measured on C3 samples with or without pretreatments (43 to 44 %). All untreated woods show high values (ranging between 47 and 53%), indicating the presence of other compounds such as extractives and lignin that have higher C %. However, wood treated with ABA and BABA procedures show higher C concentration, which is probably linked to removal of the ash that is devoid of C (Table 2). It is noteworthy that the %C results after all pretreatments incorporating a bleaching step are compatible with the cellulose range (43–45%).

Several authors have shown that different wood fractions are characterized by different $\delta^{13}\text{C}$ ‰, and that the cellulose fraction shows less negative $\delta^{13}\text{C}$ values with respect to bulk wood (Borella et al. 1998; Hoper et al. 1998; Cullen and MacFarlane 2005; Cullen and Grierson 2006; Harlow et al. 2006). Even if the $\delta^{13}\text{C}$ measurements by AMS have a rather low precision (on the order of 1 ‰ for AixMICADAS; Bard et al. 2015) the results obtained on untreated and pretreated wood clearly confirm this trend (Table 3). Indeed, all procedures incorporating a bleaching step for cellulose isolation, lead to a systematic $\delta^{13}\text{C}$ increase by up to several ‰ (the only exception is for the Quercus-1980 which, after α -cellulose extraction, remains compatible within the large $\delta^{13}\text{C}$ errors, with the untreated wood).

^{14}C results on Standards and Known-Age Woods

Figures 2–4 illustrate the results of standard C3, Quercus-1980, and Larix-1980 modern samples. Because of the expected difficulty of cellulose extraction in coniferous wood as opposed to broadleaf wood (Cullen and MacFarlane 2005), pretreatments were tested extensively on Larix-1980 with all variants of our chemical procedures (Figure 4).

The results of C3 and Larix-1980 show no difference between samples of the same material analyzed with or without chemical treatment, indicating the absence of contamination in the original materials (Figures 2 and 4). By contrast, the Quercus-1980, measured without chemical pretreatment, exhibits $F^{14}\text{C}$ results clearly lower than those of all pretreated samples, indicating a younger contamination. This could be due either to an unusual carbon translocation between rings or to artifacts acquired during tree sampling, storage or laboratory manipulation.

Overall, the results of these three modern samples show that there is no significant difference among the pretreatments, which all lead to accurate values: the IAEA certified value for C3 and clean air atmospheric values for Quercus-1980 and Larix-1980 (Figures 2–4).

Similarly, the results for the subfossil pine COUT203 measurements show no ^{14}C age difference among pretreatments, nor even for the absence of pretreatment (Figure 5). This indicates the

Table 2 Percentages of C of all samples are given for each pretreatment method. All values are followed by standard deviation of same sample/treatment replications.

	No treatment	ABA	BABA	BABAB-mod	Holo-cell	α -cellulose	BABBA1	BABBA2	ABA-B
C3	42.6 \pm 0.03	44 \pm 0.1	43.5 \pm 1	43.1 \pm 0.1	44.4 \pm 0.03	43.1 \pm 0.1	44.4 \pm 0.2	—	44.2 \pm 0.1
Quercus_1980	48.2 \pm 0.4	50.2 \pm 0.2	50.5 \pm 0.3	45.2 \pm 0.2	43.8 \pm 0.1	43 \pm 0.04	44.3 \pm 0.04	—	—
Larix_1980	48.2 \pm 0.3	52.8 \pm 0.9	53 \pm 0.7	45.1 \pm 0.2	43.4 \pm 0.2	43.8 \pm 0.1	44 \pm 0.2	44.3 \pm 0.1	43.3 \pm 0.1
COU203	46.8 \pm 0.5	49.7 \pm 0.2	49.9 \pm 0.3	43.1 \pm 0.2	43.3 \pm 0.03	43.6 \pm 0.4	43.5 \pm 0.04	43.8 \pm 0.1	43.6 \pm 0.03
Plio	47.6 \pm 3.3	55.8 \pm 1.2	57.5 \pm 0.6	43.5 \pm 0.9	43 \pm 0.3	43.2 \pm 0.05	43.8 \pm 0.1	44.1 \pm 0.4	43.9 \pm 0.4
VIRI_K	53.1 \pm 0.8	55.4 \pm 0.8	55.3 \pm 4.2	43.2 \pm 0.4	43.3 \pm 0.5	43.3 \pm 0.6	43.5 \pm 0.1	44.2 \pm 0.2	43.9 \pm 0.2

Table 3 The $\delta^{13}\text{C}$ ‰ of all samples is given for each pretreatment method. All values are followed by standard deviation of same sample/treatment replications.

	No treatment	ABA	BABA	BABAB-mod	Holo-cell	α -cellulose	BABBA1	BABBA2	ABA-B
C3	-24 \pm 0.8	-25.4 \pm 0.4	-24.7 \pm 0.6	-24.6 \pm 0.7	-23.9 \pm 1.1	-25.3 \pm 1.5	-25.7 \pm 1.2	—	-23.8 \pm 0.3
Quercus_1980	-27.1 \pm 1	-26.3 \pm 0.8	-24.9 \pm 1.7	-24 \pm 0.9	-24.8 \pm 0.7	-27.3 \pm 1	-25.8 \pm 1	—	—
Larix_1980	-26.2 \pm 0.5	-25.8 \pm 0.4	-25.8 \pm 0.4	-24.1 \pm 0.9	-23 \pm 0.1	-25.3 \pm 1	-24.6 \pm 1.4	-23.7 \pm 1.3	-21.9 \pm 0.2
COU203	-24.3 \pm 0.8	-24.7 \pm 0.4	-24.3 \pm 0.1	-21.7 \pm 0.9	-21.9 \pm 2.3	-23.5 \pm 0.4	-22.1 \pm 1.7	-22.6 \pm 1.5	-21.3 \pm 0.9
Plio	-24.9 \pm 0.8	-25 \pm 0.5	-25.2 \pm 0.8	-21.5 \pm 0.6	-21.3 \pm 1.4	-22.8 \pm 0.1	-23 \pm 1.2	-22.7 \pm 0.6	-20.7 \pm 1.8
VIRI_K	-23.7 \pm 0.7	-22.8 \pm 0.6	-22.7 \pm 0.7	-19.5 \pm 0.7	-20.2 \pm 0.7	-20.2 \pm 0.6	-19.9 \pm 1	-21.3 \pm 0.6	-21.2 \pm 0.3

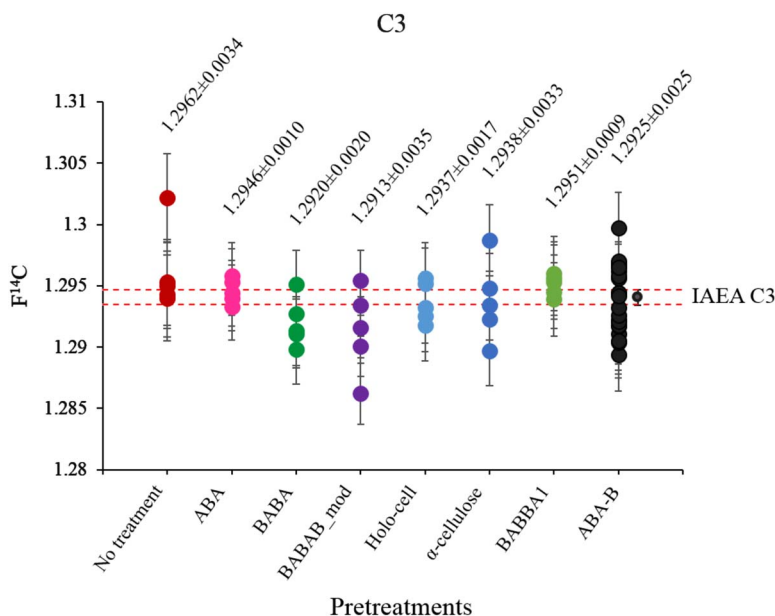


Figure 2 $F^{14}\text{C}$ analyses of the IAEA-C3 standard pretreated with different methods (error bars are $\pm 1\sigma$, including counting statistics and sample preparation uncertainties), compared with certified standard value (between dashed lines). Five ^{14}C measurements, from five samples that underwent different combustions/graphitizations, were performed for each pretreatment, with the exception of ABA-B, measured 22 times (22 different samples) from five replications of the same chemical pretreatment. For each treatment, the average value followed by the SD is indicated. For the ABA-B pretreatment, the weighted mean with its $\pm 1\sigma$ weighted error is reported in the small dot close to the series of individual $F^{14}\text{C}$ values.

lack of contamination in the original wood. Furthermore, our results are compatible with a single ^{14}C measurement performed at the Poznan AMS laboratory (Figure 5).

In summary, the replication for each pretreatment gives highly reproducible results for most samples (Figures 2–5). The only significant differences are observed for the wood blanks (Figure 6). For the Plio wood, samples measured without pretreatment and with the simplest ABA pretreatment, exhibit the largest scatter, in contrast with the results obtained with other pretreatments. The BABA and cellulose extraction procedures (with the exception of α -cellulose and ABA-B procedure) give similar results with average values ranging from 0.0025 to 0.0020 $F^{14}\text{C}$ (48,300 to 50,000 BP; Figure 6A).

As anticipated, the α -cellulose extraction is probably too aggressive for this very old and poorly preserved sample. Indeed, this procedure destroyed most of the material in two of the three extractions (see also the discussion of extraction yields, above). Moreover, our single measurement on this small-sized residual cellulose sample show a $F^{14}\text{C}$ of 0.0037, corresponding to an age of 45,000 BP. This is probably linked to an increase of the relative impact of the contamination compared to the small amount of residual carbon for this sample.

The first ABA-B pretreatment of the Plio wood was performed with one final bleaching 2-hr step, during which intense effervescence occurred. The results of three replications of this pretreatment (6 measurements) show an average value of 0.0022 $F^{14}\text{C}$ with an SD of 0.0006 (49,300 with an SD of 2500 yr BP). Three additional pretreatments were performed with two 1-hr

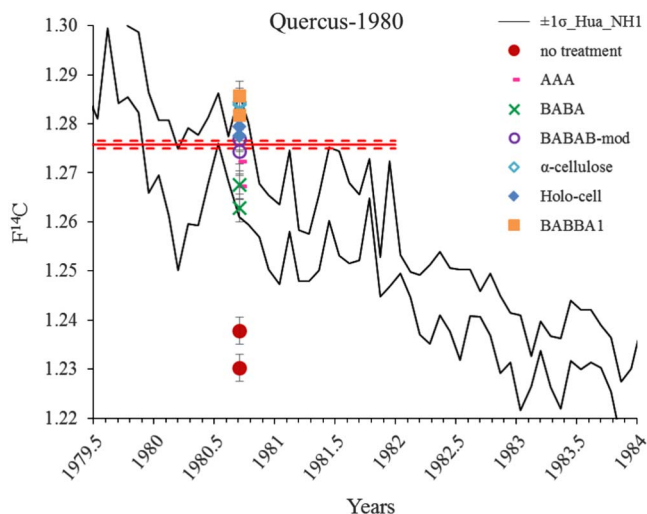


Figure 3 $F^{14}C$ content of the latewood of Quercus-1980 (error bars are $\pm 1\sigma$, including counting statistics and sample preparation uncertainties), compared with clean air $F^{14}C$ values (1σ) of the corresponding period (between solid black lines; Hua et al. 2013). Two ^{14}C measurements, from two samples that underwent different combustions/graphitizations, were performed for each pretreatment. The weighted average of all values obtained from pretreatments is the red solid line, while the corresponding $\pm 1\sigma$ weighted error is shown by dashed red lines. (Color refers to online version.)

bleaching steps instead of one bleaching step lasting 2 hr. The six new results give an average $F^{14}C$ value of 0.0015, corresponding to an age of 52,300 yr BP with an SD of 150 yr, which is better than the first ABA-B procedure (Figure 6A).

Concerning the VIRI-K blank wood (Figure 6B), untreated samples exhibit ages ranging between 0.0040 and 0.0021 $F^{14}C$ (corresponding to an age between 44,400 and 49,700 yr BP), which is older than those observed for the Plio untreated samples that range between 0.0066 and 0.0028 $F^{14}C$ (between 40,400 and 47,100 yr BP). This may be due to heterogeneities in the younger material contaminating these blank samples or may reflect a random scatter. The age results for the samples pretreated with the ABA procedure show high variability, similar to that observed for the Plio wood. The BABA pretreatment applied to VIRI-K leads to higher blank values than for Plio, while the BABAB-mod, Holo-cell and α -cellulose procedures show comparable results of about 0.0020 $F^{14}C$ (50,000 yr BP) on average. The higher scatter of α -cellulose values might be explained by increased contamination during this long pretreatment, which include many steps.

Results with the BABBA1 procedure gave an average value of 0.0030 $F^{14}C$ with an SD of 0.0009 (47,000 yr BP with an SD of 2700), a higher and more scattered blank value than for previous cellulose extraction procedures. These results were somewhat surprising, considering that BABBA1 combines the strengths of the BABAB-mod and Holo-cell methods, which both provided better blanks. The procedure was thus strengthened (BABBA2) with longer NaOH and HCl steps. The BABBA2 results exhibit a smaller scatter, but the average blank value is still rather high: 0.0029 $F^{14}C$ with an SD of 0.0004 (equivalent to 47,100 yr BP with a SD of 1000; Figure 6B) when compared to other results for this wood and to measurements obtained for

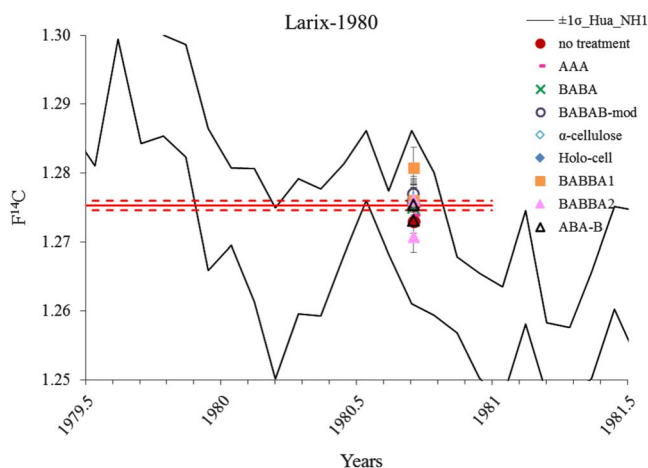


Figure 4 $F^{14}\text{C}$ content of the latewood of Larix-1980 (error bars are $\pm 1\sigma$, including counting statistics and sample preparation uncertainties), compared with clean air $F^{14}\text{C}$ values ($\pm 1\sigma$) of the corresponding period (between solid black lines; Hua et al. 2013). Two ^{14}C measurements, from two samples that underwent different combustions/graphitizations, were performed for each pretreatment. The weighted average of all values obtained from pretreatments is the red solid line, while the corresponding $\pm 1\sigma$ weighted error is shown by dashed red lines. (Color refers to online version.)

the Plio wood. An additional source of variability may also be linked to contamination during the rather long and strong BABBA procedures.

Finally, the ABA-B procedure gave excellent results with a low background average value and a rather small scatter (Figure 6B). This confirms a similar observation detected for the Plio wood measured with the same procedure. In order to further test its reproducibility, ABA-B was repeated again 9 times on VIRI-K, leading to a total of 25 measurements which gave an average value of 0.0017 with an SD of 0.0003 (corresponding to an age of 51,300 yr BP and an SD of 1500; Figure 6B).

The ABA-B procedure was thus chosen as the preferred protocol based on its precise and accurate measurements on modern, ancient and blank wood samples. This procedure is also optimal because its overall duration is shorter than most of the other procedures.

Further Validation of the Preferred Wood Pretreatment

After the phase of developments and tests described above, the preferred ABA-B procedure was used to date the wood samples distributed in the frame of the 2013 SIRI Radiocarbon Inter-comparison. The chemical extraction was performed twice for each sample and two ^{14}C measurements were generally made for each pretreatment (Table 4). C3 samples and VIRI-K blank wood, pretreated with ABA-B treatment, were used respectively as control standards and for background correction. The ^{14}C measurements performed with AixMICADAS followed the same protocol as described in the previous section, with a new convention for the background correction and error propagation: it was performed by using the average blank value obtained during the measurement session and a conservative variability of $F^{14}\text{C} = 0.0003$ (value obtained from the standard deviation of 25 VIRI-K blanks). In rare cases of blank variability

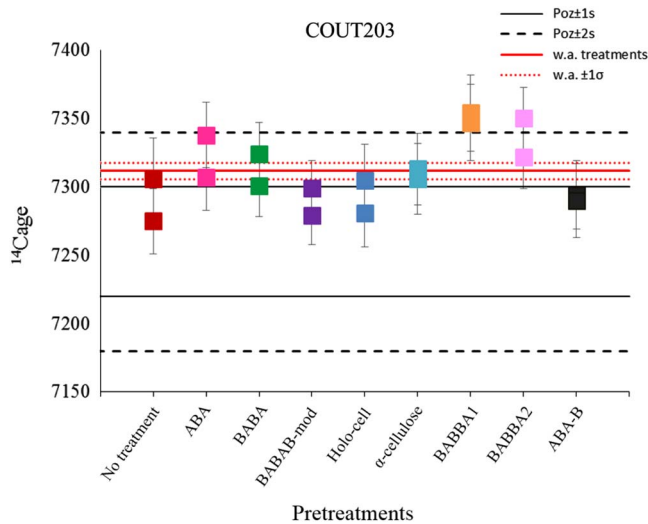


Figure 5 ¹⁴C ages of the COUT203 sample, pretreated with different methods (error bars are 1σ , including counting statistics and sample preparation uncertainties), compared with previous ¹⁴C measurements performed in the Poznan laboratory ($\pm 1\sigma$ value between solid black lines; $\pm 2\sigma$ between dashed black lines). Two ¹⁴C measurements, from 2 samples that underwent different combustions/graphitizations, were performed for each pretreatment. The weighted average of all values obtained from pretreatments is the red solid line, while the corresponding $\pm 1\sigma$ weighted error is shown by dotted red lines. (Color refers to online version.)

larger than $F^{14}\text{C} = 0.0003$ during a particular session, the measured variability during the session is used instead for the error calculation.

Table 4 provides the weighted means and errors for the different samples, in comparison with average results from the SIRI intercomparison (Scott et al. 2016). Our results are in very good agreement with the SIRI results, which further validate our choice of the ABA-B pretreatment.

II. DATING A PINE SEQUENCE BELONGING TO THE YOUNGER DRYAS EVENT

STUDY AREA AND CONTEXT

In the region of the upper course of the Durance River in the Southern French Alps, many subfossil woods (*Pinus sylvestris* L.) were discovered in alluvial sediments dated from Late Glacial to the first part of the Holocene (Miramont et al. 2000). Since the end of the last glacial period, the rivers of this region have been characterized by alluvial detrital phases, interrupted by periods of river incision. Pines were buried by floods during these sedimentation phases. Marl soils allowed the very good preservation of these subfossil stems, which were sometimes preserved with their bark. These subfossil pines were subsequently revealed by the modern incision of the rivers.

Eighteen subfossil stems were discovered in the Barbiers River alluvium in the region of Sisteron. Because of the geomorphological stress and the harshness of the mountain climate, which is reinforced by the intensity and irregularity of the Mediterranean rainfall regime, tree growth was characterized by many anomalies, which made it difficult to synchronize all sequences with their dendrochronological patterns (Miramont et al. 2011). So far, only a few trees have been grouped into two floating chronologies: BARB-A and BARB-B (Miramont et al. 2011).

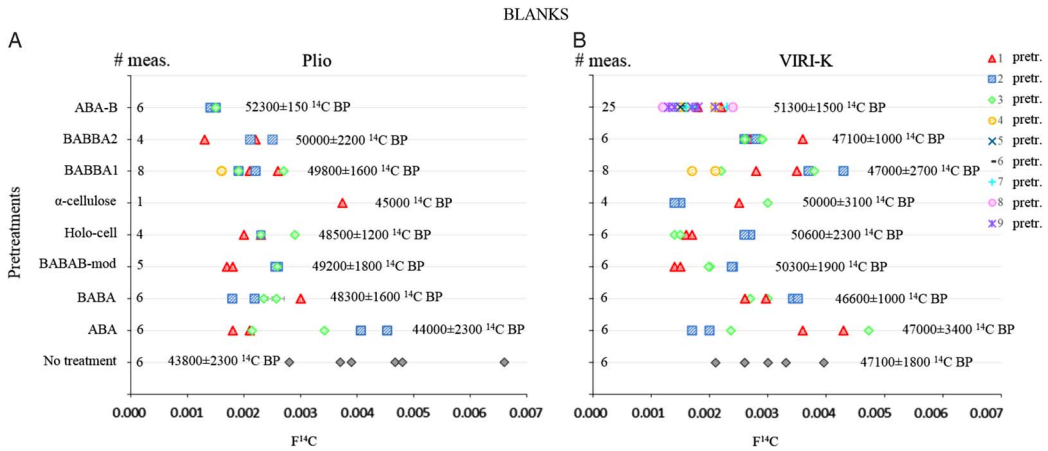


Figure 6 ¹⁴C content of blank samples (A: Plio; B: VIRI-K) pretreated with different methods (error bars are 1σ). Different pretreatments (pretr.) were performed for each method (i.e. 1 pretr., 2 pretr., etc. indicate the specific—first, second, etc.—replication of each pretreatment: ABA, BABA, etc.) and two AMS measurements were performed for each pretreatment, when enough material was available. The only exception is VIRI-K treated with ABA-B, which was measured more than twice for each pretreatment. The total numbers of measurements (# meas.) are given for each method at the beginning of each line of the Figure, as well as the ¹⁴C age average with SD. No background correction has been subtracted.

Table 4 Results of the Sixth International Radiocarbon Intercomparison (SIRI) 2013: official Intercomparison results (Scott et al 2016) and our results with relative 1σ uncertainty (¹⁴C age and F¹⁴C). The number of measurements determined in Aix-en-Provence is indicated in the last column.

Sample	SIRI ¹⁴ C		Aix ¹⁴ C		F ¹⁴ C	1σ error	Nr of meas.
	age BP	1σ error	age BP	1σ error			
SIRI A	51,697 ^a	—	48,631 ^b	163	0.0024 ^b	0.0001	4
			>58,000 ^c	—	0.0004 ^c	0.0002	
SIRI E	10827	77	10,887	16	0.2579	0.0005	4
SIRI F	370	34	391	10	0.9526	0.0012	4
SIRI G	378	40	388	10	0.9527	0.0012	4
SIRI H	385	36	387	10	0.953	0.0011	4
SIRI I	9987	49	10,027	17	0.287	0.0006	3
SIRI L	50,195 ^a	—	48,688 ^b	148	0.0023 ^b	0.0001	4
			>59,000 ^c	—	0.0003 ^c	0.0002	

^a¹⁴C finite age after blank subtraction.

^bWeighted means of ¹⁴C age without blank subtraction.

^cWeighted means of ¹⁴C age after blank subtraction (the F¹⁴C of mean blank is 0.0023 ± 0.0003 and 0.0016 ± 0.0003, respectively, for the two magazines of graphite targets). These conventional age values are calculated following van der Plicht and Hogg (2006), who recommend to using F¹⁴C = F¹⁴C + 2 σ when F¹⁴C < 2 σ.

Preliminary ¹⁴C ages were used to tentatively place these trees on the absolute dendrochronological timescale (Kaiser et al. 2012).

MATERIALS AND METHODS

The trees selected for this study are Barb12 and Barb17. Barb12 has a sequence of 210 rings that are narrow at the end of the sequence; while Barb17 has a sequence of 167 rings that are very

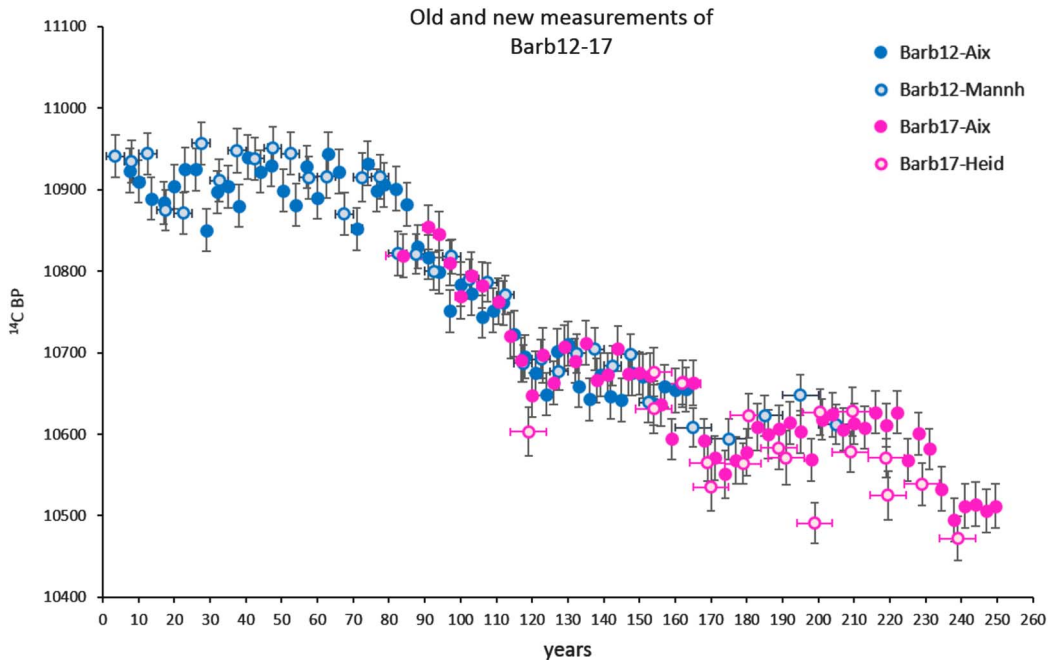


Figure 7 Comparison between ^{14}C measurements on the Barb12 and Barb17 trees performed in Germany (Mannheim and Heidelberg; Miramont et al. 2011; Kaiser et al. 2012) and in Aix-en-Provence. The vertical bars indicate 1σ sample uncertainty (including counting statistics and sample preparation uncertainties), while the horizontal bars indicate the number of rings included in each measured sample. Almost all Aix samples have annual resolution.

narrow at the beginning and the end of the sequence. While Barb12 is included into BARB-A chronology, Barb17 is not. A preliminary synchronization of Barb17 with the other trees of BARB-A was proposed by Miramont et al. (2011), but the quality of the dendro-correlation resulted in its exclusion from the BARB-A chronology. For the present work, a new slice was cut from the same stem with a total length of 173 rings. Five additional rings were discovered at the beginning of the new sequence (considered to be the pith). Following the former dendrochronological sequence, the five new rings were counted with negative numbers (from -5 to -1). For the Barb12 tree, only the initial clear sequence of 163 rings has been analyzed.

The new sequences were sampled at annual resolution when permitted by the ring width, by using a scalpel and with the help of a binocular microscope (Figure 7, Table 5). As a first step, every third ring was pretreated for ^{14}C analysis. These samples were sliced in small pieces and pretreated by using the ABA-B method (as described and tested in the first part of this work) before being combusted, graphitized with the AGE system and measured with AixMICADAS.

High precision ^{14}C measurements were performed with long AMS runs to reach at least 800,000 ion counts for each OxA2 standards on the same magazine. In addition, C3 and VIRI-K samples were pretreated and measured in the same batch, serving as control modern standard and blank. As for other wood samples, an additional uncertainty of 1.6% was propagated in the ^{14}C analytical errors and background correction followed the convention described above in the section on SIRI samples.

Table 5 ^{14}C ages measured on the Barb12-17 sequence.

Lab code	Tree	Ring nr	Middle ring rel. sequence	^{14}C age	1σ error
11068.1.1	Barb12	7–8	7.5	10,923	27
11069.1.1	Barb12	9–11	10	10,910	26
11070.1.1	Barb12	13–14	13.5	10,889	26
11071.1.1	Barb12	17	17	10,884	26
11072.1.1	Barb12	20	20	10,904	27
11073.1.1	Barb12	23	23	10,925	27
11074.1.1	Barb12	26	26	10,925	26
11075.1.1	Barb12	29	29	10,850	26
11076.1.1	Barb12	32	32	10,897	26
11077.1.1	Barb12	35	35	10,904	26
11078.1.1	Barb12	38	38	10,880	26
11079.1.1	Barb12	40–41	40.5	10,940	27
11080.1.1	Barb12	44	44	10,922	26
11081.1.1	Barb12	47	47	10,930	26
11082.1.1	Barb12	50–51	50.5	10,899	26
11083.1.1	Barb12	54	54	10,881	26
11084.1.1	Barb12	57	57	10,928	26
11085.1.1	Barb12	60	60	10,890	26
11086.1.1	Barb12	63	63	10,944	27
11087.1.1	Barb12	66	66	10,922	27
11088.1.1	Barb12	70–72	71	10,852	26
11089.1.1	Barb12	73–75	74	10,932	27
11090.1.1	Barb12	76–77	76.5	10,899	26
11091.1.1	Barb12	78–79	78.5	10,906	27
11092.1.1	Barb12	82	82	10,901	27
11093.1.1	Barb12	85	85	10,882	27
11094.1.1	Barb12	88	88	10,830	26
11095.1.1	Barb12	91	91	10,817	27
11096.1.1	Barb12	94	94	10,799	27
11097.1.1	Barb12	97	97	10,751	26
11098.1.1	Barb12	100	100	10,784	27
11099.1.1	Barb12	103	103	10,773	27
11100.1.1	Barb12	106	106	10,744	26
11101.1.1	Barb12	109	109	10,752	27
11102.1.1	Barb12	112	112	10,761	27
11103.1.1	Barb12	115	115	10,723	28
11104.1.1	Barb12	118	118	10,695	27
11105.1.1	Barb12	121	121	10,675	27
11106.1.1	Barb12	124	124	10,649	26
11107.1.1	Barb12	127	127	10,702	27
11108.1.1	Barb12	130	130	10,711	27
11109.1.1	Barb12	133	133	10,659	26
11110.1.1	Barb12	136	136	10,643	26
11111.1.1	Barb12	139	139	10,673	27
11112.1.1	Barb12	142	142	10,646	27
11113.1.1	Barb12	145	145	10,642	27
11114.1.1	Barb12	148	148	10,675	27

Table 5 (Continued)

Lab code	Tree	Ring nr	Middle ring rel. sequence	¹⁴ C age	1 σ error
11115.1.1	Barb12	151	151	10,671	27
11116.1.1	Barb12	154	154	10,638	27
11117.1.1	Barb12	157	157	10,659	26
11118.1.1	Barb12	160	160	10,654	27
11119.1.1	Barb12	163	163	10,655	27
11067.1.1	Barb17	-5/5	84	10,819	27
11066.1.1	Barb17	6-8	91	10,854	27
11065.1.1	Barb17	9-11	94	10,845	28
11064.1.1	Barb17	12-14	97	10,810	28
11063.1.1	Barb17	15-17	100	10,769	27
11062.1.1	Barb17	18-20	103	10,795	28
11061.1.1	Barb17	21-23	106	10,783	28
11060.1.1	Barb17	26-27	110.5	10,763	28
11059.1.1	Barb17	30	114	10,721	28
11058.1.1	Barb17	33	117	10,691	27
11057.1.1	Barb17	36	120	10,648	27
11056.1.1	Barb17	39	123	10,697	34
11055.1.1	Barb17	42	126	10,663	27
11054.1.1	Barb17	45	129	10,707	27
11053.1.1	Barb17	48	132	10,690	27
11052.1.1	Barb17	51	135	10,712	27
11051.1.1	Barb17	54	138	10,666	27
11050.1.1	Barb17	57	141	10,673	27
11049.1.1	Barb17	60	144	10,705	28
11048.1.1	Barb17	63	147	10,674	26
11047.1.1	Barb17	66	150	10,675	26
11046.1.1	Barb17	69	153	10,672	27
11045.1.1	Barb17	72	156	10,636	26
11044.1.1	Barb17	75	159	10,594	25
11043.1.1	Barb17	78	162	10,664	27
11042.1.1	Barb17	81	165	10,663	28
11041.1.1	Barb17	84	168	10,592	27
11040.1.1	Barb17	87	171	10,571	27
11039.1.1	Barb17	90	174	10,551	29
11038.1.1	Barb17	93	177	10,568	29
11037.1.1	Barb17	96	180	10,578	29
11036.1.1	Barb17	99	183	10,609	29
11035.1.1	Barb17	102	186	10,600	30
11034.1.1	Barb17	105	189	10,607	28
11033.1.1	Barb17	108	192	10,614	26
11032.1.1	Barb17	111	195	10,603	26
11031.1.1	Barb17	114	198	10,569	26
11030.1.1	Barb17	117	201	10,618	25
11029.1.1	Barb17	120	204	10,624	27
11028.1.1	Barb17	123	207	10,606	26
11027.1.1	Barb17	126	210	10,613	25
11026.1.1	Barb17	129	213	10,608	26

Table 5 (Continued)

Lab code	Tree	Ring nr	Middle ring rel. sequence	^{14}C age	1σ error
11025.1.1	Barb17	132	216	10,627	26
11024.1.1	Barb17	135	219	10,611	27
11023.1.1	Barb17	138	222	10,627	26
11022.1.1	Barb17	141	225	10,568	26
11021.1.1	Barb17	144	228	10,601	26
11020.1.1	Barb17	147	231	10,582	25
11123.1.1	Barb17	150–151	234.5	10,533	27
11124.1.1	Barb17	154	238	10,495	27
11125.1.1	Barb17	157	241	10,512	27
11126.1.1	Barb17	160	244	10,514	27
11127.1.1	Barb17	163	247	10,506	27
11128.1.1	Barb17	165–166	249.5	10,512	27

High-Resolution ^{14}C Results on the Barb12-17 Trees

The new ^{14}C data measured on selected annual rings from the Barb12-17 sequence can be compared with previous measurements: for the Barb17, previous measurements were performed on decadal samples (i.e. large samples mixing the wood of specific decades) performed by β -counting on CO_2 in Heidelberg; while for the Barb12, the sequence was analyzed on five-year samples until ring 155, then on decadal samples by the AMS facility of Mannheim (Miramont et al. 2011; Kaiser et al. 2012). Figure 7 illustrates the very good agreement between the old and new datasets, generally well within the one sigma error bars. The Barb17 ^{14}C record can also be compared with other tree-ring sequences of the Younger Dryas period (Figure 8), as follows:

- The CELM chronology is a floating 1606-yr chronology composed of Swiss and German pines (Kaiser et al. 2012). The youngest tree of the sequence, G5, has been dated in several works from ca. 12,500 to $12,844 \pm 32$ cal BP (Hughen et al 2000; Muscheler et al 2008; Hua et al 2009; Bronk Ramsey et al 2012).
- The Swiss YDB chronology, which is the oldest part of the absolute dendrochronological chronology. For the IntCal13 ^{14}C calibration curve (Reimer et al. 2013) the YDB started at 12,594 cal BP based on published studies (Schaub et al. 2008; Hua et al. 2009; Kaiser et al. 2012), but more recent work has shown that the YDB sequence remains floating and the absolute dendrochronological series only ends at 12,325 cal BP (M. Friedrich, IntCal dendro-meeting in Zürich, August 2015; Kromer et al. 2015).
- The Kauri (*Agathis australis*) chronology, which is based on trees from New Zealand, and spans the period between ca. 11,694 and 13,134 cal BP without interruption. Despite the interhemispheric ^{14}C gradient (see discussion below), the overlap with the absolute ^{14}C series over ca. 200 years (ca. 11,694–11,900 cal BP) enabled Hogg et al. (2016a, 2016b) to date the Kauri sequence precisely. In turn, the Kauri chronology has been used to connect the Swiss YDB and German/Swiss CELM sequences, extending the tree-ring record back to $14,174 \pm 3$ cal BP (Hogg et al. 2016a, 2016b).

In Figure 9, the new Barb17 sequence is matched against the YDB (Kaiser et al. 2012) and the Kauri chronologies (Hogg et al. 2016a). Assuming that the floating Kauri series is dated

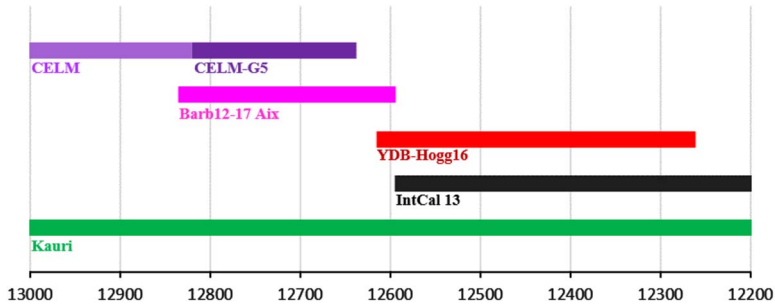


Figure 8 Comparison between the tree-ring sequences of the Younger Dryas period. The YDB chronology, included in the IntCal13 curve, recently became floating (see text for details). In this figure we report the new position proposed by Hogg et al. (2016b). The Barb12-17 sequence is shown in its entire length (12,836–12,594 cal BP). The CELM chronology ends with tree G5. We decided to exclude tree G3, as other studies have done, because of the absence of published dendrochronological synchronization between this tree and CELM chronology. Overall, this figure illustrates the importance of the tree Barb17 tree in connecting the YDB and CELM chronologies.

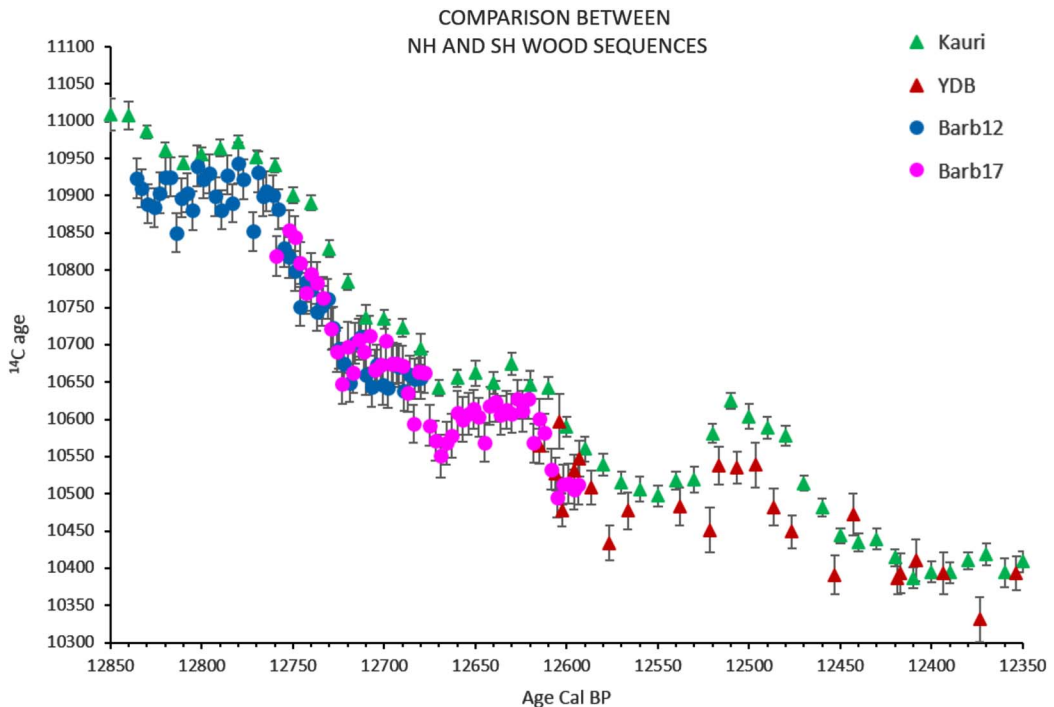


Figure 9 Matching between available tree-ring sequences for the Younger Dryas period: for the Northern Hemisphere (NH), the Barb17 tree in pink, the Barb12 in blue and YDB in red (Hua et al. 2009); for the Southern Hemisphere (SH), the Kauri tree in green (Hogg et al. 2016) without interhemispheric gradient correction. Error bars are given at 1σ . (Colors refer to online version.)

accurately, we dated our Barb12-17 ^{14}C sequence from about 12,836 to 12,594 cal BP. This preliminary dating was performed by visual tuning, considering especially the peak around 12,670 cal BP, which is present in both Barbiers from the Northern Hemisphere (NH) and the

Kauri record from the Southern Hemisphere (SH; Figure 9). This global feature probably represents a solar event. Based on the new ^{14}C dataset, the proposed dating shifts the Barb17 sequence towards an age older than previously thought (Miramont et al. 2011). Interestingly, the new ^{14}C series for Barb12 and Barb17 provides support for a previous unpublished dendrochronological overlap, which was not considered sufficiently robust based on its statistical values (GIK = 56%; TBP = 4.0; TH = 6.1 and CDI = 25). Overall, this confirms the usefulness of the annual resolution sampling for a more precise synchronization.

The proposed date for Barb12-17 seems to be confirmed by the ca. 24-yr overlap with YDB chronology (Figure 9). Based on the comparison with our new Barb12-17 sequence, the last sample of tree G5 of the CELM chronology can be dated to ca. 12,635 cal BP (Figure 8).

$^{14}\text{CO}_2$ Atmospheric Interhemispheric Gradient

It is widely recognized that there is a small, but systematic ^{14}C difference between wood from trees that lived at the exact same time in the northern and southern hemispheres (SH wood being consistently older than NH wood). This interhemispheric gradient (IHG) is maintained principally by the air-sea CO_2 exchange with the ocean surface that is typically much older than the atmosphere (from 400 to 1200 yr; Bard 1988). Indeed, there is proportionally more ocean surface in the SH than in the NH, and the Southern Ocean is also characterized by generalized upwelling of old water and intense CO_2 piston velocity due to extreme winds in the 40° to 60°S latitude belt (Levin et al. 1987; Braziunas et al. 1995). The situation is even more complex for recent trees because the IHG has been perturbed and reversed by the anthropogenic injection of fossil CO_2 mainly in the NH (Stuiver and Braziunas 1998; McCormac et al. 1998).

Precise measuring of the IHG and of its possible variations through time is thus of prime interest to studying the global carbon cycle. Hogg et al. (2016a, 2016b) used ^{14}C data measured in trees from the NH and SH to calculate the IHG during most of the Younger Dryas climatic event. The new Barb12-17 dataset from Southern France compared to the Kauri sequence from New Zealand can be used to estimate new IHG values for a ca. 220-yr interval that occurred during the Younger Dryas event.

A difficulty arises from the different resolution of the two records: the Kauri record is based on ^{14}C replicates of wood homogenized over specific decades, whereas our Barb12-17 record is based on single-year wood dated every 3 yr. This latter record thus contains inter-annual noise linked to various effects on the ^{14}C production and carbon cycle. Indeed, based on ^{14}C analyses at annual resolution over the past 500 yr, Stuiver and Braziunas (1993, 1998) evidenced significant spectral power for frequencies close to or lower than 10 yr, which should be present in the Barb12-17 record, but are inevitably smoothed out in the Kauri record. In order to reduce the inter-annual variability, we thus smoothed the Barb12-17 record with a Gaussian low-pass filter with a sigma of 3 yr. For Barb12-17, the smoothed values corresponding to individual analyzed samples were then grouped and averaged over the same decades as in the Kauri record. In order to fully take into account analytical uncertainties, the original measurement errors were used in the error propagation when calculating for each decade a weighted average and error of Barb12-17 samples. This conservative procedure has been used in Figure 10 to compare the Barb and Kauri records.

Twenty-three values of the ^{14}C IHG can be calculated by subtracting the Barb12-17 smoothed ^{14}C ages from the corresponding Kauri decadal ^{14}C averages (Figure 9). The mean IHG value is 65 yr with a SD of 20 yr.

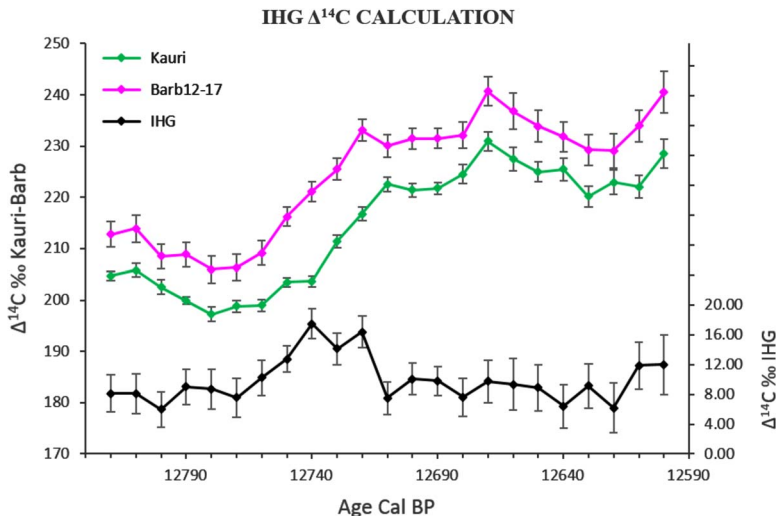


Figure 10 Comparison between Kauri and Barb12-17 $\Delta^{14}\text{C}\text{‰}$ records. The average difference associated with the IHG is given in the black line in the bottom of the graphic (y-axis on the right).

As shown in Figure 10, the IHG almost doubles during the drastic rise of $\Delta^{14}\text{C}\text{‰}$ (i.e. 12,750–12,720 cal BP). Interestingly this transient IHG maximum occurs during the rapid 25‰ $\Delta^{14}\text{C}$ rise starting at 12750 cal BP and stabilizing around 12,710 cal BP. More work is needed to understand the cause of this 25‰ $\Delta^{14}\text{C}$ rise, notably comparing the ^{14}C record with those based on other cosmogenic nuclides (e.g. ^{10}Be in polar ice). Numerical modeling would also help studying the delayed response of the Southern Hemisphere.

For the general comparison shown in Figure 11, we excluded this transient period in the IHG average calculation. The new mean IHG value is 57 yr with a SD of 11 yr, with an IHG maximum value (100 yr with a SD of 14 yr based on four values) during the drastic $\Delta^{14}\text{C}\text{‰}$ rise. In Figure 11, the Kauri record is corrected by subtracting 57 yr in order to illustrate the agreement between the Kauri and Barb12-17 records.

The IHG can also be calculated in terms of $\Delta^{14}\text{C}$ unit: the total mean value is 10‰ with a SD of 3‰ (Figure 10); the value without 12,750–12,720 cal BP period is 9‰ with a SD of 2‰; finally the value during the 12,750–12,720 cal BP period is 15‰ with a SD of 2‰.

Our IHG determination is expected to be particularly robust during the 12,660–12,620 and 12,820–12,760 cal BP intervals because the individual ^{14}C records exhibit so-called “age plateaus.” Indeed, over 12,660–12,620 cal BP the IHG average is 52 yr with a SD of 10 yr based on four individual Kauri-Barb12-17 comparisons included in this ^{14}C plateau; while during the 12,820–12,760 cal BP interval the IHG average is 55 yr with a SD of 9 yr for the seven individual Kauri-Barb12-17 comparisons included in this plateau. Shifting the calendar age of the Barbiers curve with respect to the Kauri record would leave the interhemispheric ^{14}C offset almost unchanged, precisely because of the presence of the same ^{14}C “age plateau” in both records.

This indicates that the IHG remained significant during this early stage of the YD event with a value close to the modelled preanthropogenic IHG (56 yr with a SD of 24 yr based on the last 500-yr mean; McCormac et al. 2004). Our IHG reconstruction agrees with that by

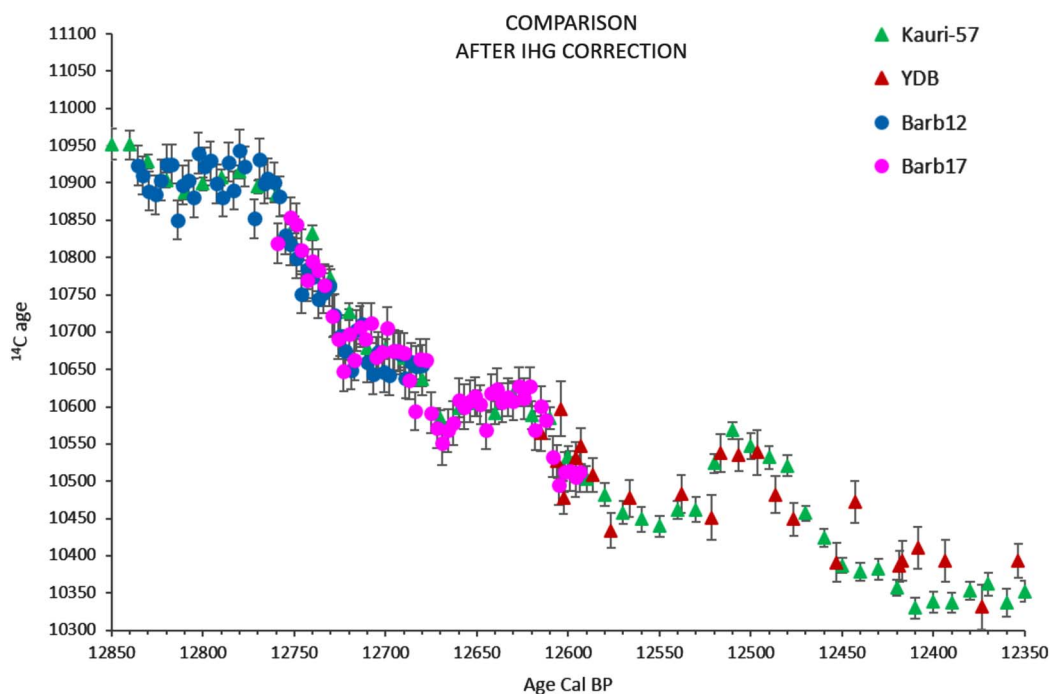


Figure 11 Comparison between Kauri, YDB, Barb12, and Barb17 sequences, after subtracting 57 yr from Kauri ^{14}C ages to correct for the interhemispheric gradient (IHG).

Hogg et al. (2016a) over the 12,650–12,620 cal BP plateau, but it differs for the 12,820–12,760 cal BP plateau, for which we find no evidence for an IHG collapse.

CONCLUSIONS AND PERSPECTIVES

The capacity to date wood has been established in the new ^{14}C laboratory in Aix-en-Provence equipped with AixMICADAS and an automated graphitization system. In this study, different chemical pretreatments are tested on wood samples of known ages. The tested protocols vary from the simple ABA technique to more elaborate protocols for cellulose purification.

All pretreatments are efficient for dating pure cellulose (IAEA-C3 standard) and various wood samples, ranging from modern woods to a subfossil sample around 7000 yr BP. By contrast, different performances are observed for old woods reaching the ^{14}C limit (“blank wood”). This is due to varying efficiencies of the contamination removal among protocols. We obtain the oldest and most reproducible ^{14}C results with holocellulose extraction procedures.

The acid-base-acid-bleaching pretreatment (ABA-B) is selected as an optimal choice based on its limited duration and complexity, and because of the excellent and reproducible analytical results (as shown by ^{14}C results, $^{13}\text{C}/^{12}\text{C}$ ratios, carbon % and overall mass yield %) that it ensures.

The efficiency of the ABA-B protocol is highlighted through the analysis of wood samples of the Sixth International Radiocarbon Intercomparison (SIRI). Our results are in good agreement with consensus values obtained by the SIRI participants.

The new method is applied to a ca. 240-yr-long tree-ring sequence from two subfossil pines (Barb12-17) collected in the southern French Alps and dated to the Younger Dryas cold period. The new ^{14}C analyses at high resolution (every third year) agree well with high-precision results obtained previously. Barb12-17 is tentatively dated to the interval between 12,836 and 12,594 cal BP by matching its ^{14}C pattern to the Kauri and YDB chronologies.

A mean IHG value of 57 yr with a SD of 11 yr is derived from the comparison with the Kauri sequence from New Zealand. The IHG stayed relatively high throughout the studied period, without evidence of a collapse around 12,800 cal BP. The IHG exhibits a transient maximum during the 12,750–12,710 cal BP interval. This period corresponds to a global rise of atmospheric $\Delta^{14}\text{C}$ but with an apparent delay in the Southern Hemisphere. Future work will be focused on additional trees from the YD period and on complementary records from other archives for both ^{14}C and ^{10}Be .

ACKNOWLEDGMENTS

AixMICADAS was acquired and is operated in the framework of the EQUIPEX project ASTER-CEREGE (PI E Bard) with additional matching funds from the Collège de France, which also supports the salaries of the authors from CEREGE. Our work on subfossil wood is also supported by the ANR project CARBOTRYDH (PI E Bard). We are grateful to Marian Scott for providing the SIRI samples, to Tomasz Goslar for ^{14}C age value of COUT203 and information about sample preparation, and to Jean Claude Hippolyte for the Pliocene wood.

REFERENCES

- Anchukaitis KJ, Evans MN, Lange T, Smith DR, Leavitt SW, Schrag DP. 2008. Consequences of a rapid cellulose extraction technique for oxygen isotope and radiocarbon analyses. *Analytical Chemistry* 80(6):2035–41.
- Bard E. 1988. Correction of accelerator mass spectrometry ^{14}C ages measured in planktonic foraminifera: paleoceanographic implications. *Paleoceanography* 3:635–45.
- Bard E, Tuna T, Fagault Y, Bonvalot L, Wacker L, Fahrni S, Synal H-A. 2015. AixMICADAS, the accelerator mass spectrometer dedicated to ^{14}C recently installed in Aix-en-Provence, France. *Nuclear Instruments and Methods in Physics Research B* 361:80–86.
- Borella S, Leuenberger M, Saurer M, Siegwolf R. 1998. Reducing uncertainties in $\delta^{13}\text{C}$ analysis of tree rings: pooling, milling, and cellulose extraction. *Journal of Geophysical Research Atmospheres* 1031(D16):19519–26.
- Braziunas TF, Fung IY, Stuiver M. 1995. The pre-industrial atmospheric $^{14}\text{CO}_2$ latitudinal gradient as related to exchanges among atmospheric oceanic and terrestrial reservoirs. *Global Biogeochemical cycles* 9:565–84.
- Brendel O, Iannetta PPM, Stewart D. 2000. A rapid and simple method to isolate pure alpha-cellulose. *Phytochemical Analysis* 11:7–10.
- Bronk Ramsey C, Staff RA, Bryant CL, Brock F, Kitagawa H, van der Plicht J, Schlolaut G, Marshall MH, Brauer A, Lamb HF, Payne RL, Tarasov PE, Haraguchi T, Gotanda K, Yonenobu H, Yokoyama Y, Tada R, Nakagawa T. 2012. A complete terrestrial radiocarbon record for 11.2 to 52.8 kyr B.P. *Science* 338:370–4.
- Bruhn F, Duhr A, Grootes PM, Mintrop A, Nadeau M. 2001. Chemical removal of conservation substances by “Soxhlet”-type extraction. *Radiocarbon* 43(2A):229–37.
- Cain WF, Suess HE. 1976. Carbon-14 in tree rings. *Journal of Geophysical Research – Oceans and Atmospheres* 81(21):3688–94.
- Capano M, Marzaioli F, Sirignano C, Altieri S, Lubritto C, D’Onofrio A, Terrasi F. 2010. ^{14}C AMS measurements in tree rings to estimate local fossil CO_2 in Bosco Fontana forest (Mantova, Italy). *Nuclear Instruments and Methods in Physics Research B* 268(7–8):1113–6.
- Capano M, Marzaioli F, Passariello I, Pignatelli O, Martinelli N, Gigli S, Gennarelli I, De Cesare N, Terrasi T. 2012. Preliminary radiocarbon analyses of contemporaneous and archaeological wood from the Ansanto Valley (southern Italy). *Radiocarbon* 54(3):701–14.
- Capano M, Altieri S, Marzaioli F, Sirignano C, Pignatelli O, Martinelli N, Passariello I, Sabbarrese C, Ricci P, Gigli S, Terrasi F. 2013. Widespread fossil CO_2 in the Ansanto Valley (AV – Italy): dendrochronological, ^{14}C and ^{13}C analyses on tree rings. *Radiocarbon* 55(2–3):1114–22.
- Cross CF, Bevan EJ. 1912. *Researches on Cellulose* 3. London.
- Cullen LE, MacFarlane C. 2005. Comparison of cellulose extraction methods for analysis of stable

- isotope ratios of carbon and oxygen in plant material. *Tree Physiology* 25:563–9.
- Cullen LE, Grierson PF. 2006. Is cellulose extraction necessary for developing stable carbon and oxygen isotopes chronologies from *Callitris glaucophylla*? *Palaeogeography, Palaeoclimatology, Palaeoecology* 236:206–16.
- Dee MW, Brock F, Bowles AD, Bronk Ramsey C. 2011. Using a silica substrate to monitor the effectiveness of radiocarbon pretreatment. *Radiocarbon* 53(4):705–11.
- de Vries H, Barendsen GW. 1954. Measurements of age by the carbon-14 technique. *Nature* 174:1138–41.
- Fedi ME, Caforio L, Liccioli L, Mandò PA, Salvini A, Taccetti F. 2014. A simple and effective removal procedure of synthetic resins to obtain accurate radiocarbon dates of restored artworks. *Radiocarbon* 56(3):969–79.
- Fengel D, Wegener G. 1989. *Wood: Chemistry, Ultrastructure, Reactions*. Berlin & New York: W de Gruyter.
- Gaudinski JB, Dawson TE, Quideau S, Schuur EA, Roden JS, Drumbore SE, Sandquist DR, Oh SW, Wasylishen RE. 2005. Comparative analysis of cellulose preparation techniques for use with ^{13}C , ^{14}C , and ^{18}O isotopic measurements. *Analytical Chemistry* 77(22):7212–24.
- Gray J, Thompson P. 1977. Climatic information from $^{18}\text{O}/^{16}\text{O}$ analysis of cellulose, lignin and whole wood from tree rings. *Nature* 270:708–9.
- Green JW. 1963. Wood cellulose. In: Whistler RL, editor. *Methods in Carbohydrate Chemistry*. Volume III. New York: Academic Press. p 9–21.
- Harlow BA, Marshall JD, Robinson AP. 2006. A multi-species comparison of $\delta^{13}\text{C}$ from whole wood, extractive-free wood and holocellulose. *Tree Physiology* 26(6):767–74.
- Hogg A, Southon J, Turney C, Palmer J, Bronk Ramsey C, Fenwick P, Boswijk G, Friedrich M, Helle G, Hughen K, Jones R, Kromer B, Noronha A, Reynard L, Staff R, Wacker L. 2016a. Punctuated shutdown of Atlantic meridional overturning circulation during Greenland Stadial 1. *Nature–Scientific Report* 6:25902.
- Hogg A, Southon J, Turney C, Palmer J, Bronk Ramsey C, Fenwick P, Boswijk G, Büntgen U, Friedrich M, Helle G, Hughen K, Jones R, Kromer B, Noronha A, Reinig F, Reynard L, Staff R, Wacker L. 2016b. Decadally resolved lateglacial radiocarbon evidence from New Zealand Kauri. *Radiocarbon* 58(4):709–33.
- Hoper ST, McCormac FG, Hogg AG, Higham TG, Head MJ. 1998. Evaluation of wood pretreatments on oak and cedar. *Radiocarbon* 40(1): 45–50.
- Hua Q, Barbetti M, Fink D, Kaiser KF, Friedrich M, Kromer B, Levchenko VA, Zoppi U, Smith AM, Bertuch F. 2009. Atmospheric ^{14}C variations derived from tree rings during the early Younger Dryas. *Quaternary Science Reviews* 28(25–26):2982–90.
- Hua Q, Barbetti M, Rakowski AZ. 2013. Atmospheric radiocarbon for the period 1950–2010. *Radiocarbon* 55(4):2059–72.
- Hughen K, Southon J, Lehman S, Overpeck T. 2000. Synchronous radiocarbon and climate shifts during the last deglaciation. *Science* 290:1951–4.
- Kaiser KF, Friedrich M, Miramont C, Kromer B, Sgier M, Schaub M, Boeren I, Remmele S, Talamo S, Guibal F, Sivan O. 2012. Challenging process to make the Lateglacial tree-ring chronologies from Europe absolute – an inventory. *Quaternary Science Reviews* 36:78–90.
- Kromer B, Manning SW, Friedrich M, Talamo S, Trano N. 2010. ^{14}C Calibration in the 2nd and 1st millennia BC—Eastern Mediterranean Radiocarbon Comparison Project (EMRCP). *Radiocarbon* 52(3):875–86.
- Kromer B, Friedrich M, Talamo S. 2015. Progress Report on Dendrochronology and ^{14}C of the Hohenheim Preboreal/YD and Late Glacial Pine chronologies. *Zürich IntCal-Dendro Meeting, Zürich, August 4–5*.
- Leavitt SW, Danzer SR. 1993. Method for batch processing small wood samples to holocellulose for stable-carbon isotope analysis. *Analytical Chemistry* 65(1):87–9.
- Levin I, Kromer B, Wagenbach D, Munnich KO. 1987. Carbon isotope measurements of atmospheric CO_2 at a coastal station in Antarctica. *Tellus* 39B(1–2):89–95.
- Li Q, Liu Y. 2013. A simple and rapid preparation of pure cellulose confirmed by monosaccharide compositions, ^{13}C , yields and C%. *Dendrochronologia* 31:273–8.
- Liu Z, Sun X, Hao M, Huang C, Xue Z, Mu T. 2015. Preparation and characterization of regenerated cellulose from ionic liquid using different methods. *Carbohydr. Polym.* 117:99–105.
- Loader NJ, Robertson I, Barker AC, Switsur VR, Waterhouse JS. 1997. An improved technique for the batch processing of small wholewood samples to α -cellulose. *Chemical Geology* 136(3):313–17.
- MacFarlane C, Warren CR, White DA, Adams MA. 1999. A rapid and simple method for processing wood to crude cellulose for analysis of stable carbon isotopes in tree rings. *Tree Physiology* 19(12):831–5.
- McCormac FG, Hogg AG, Higham TG, Baillie ML, Palmer JG, Xiong L, Pilcher JR, Brown D, Hoper ST. 1998. Variations of radiocarbon in tree rings: Southern Hemisphere offset preliminary results. *Radiocarbon* 40(3):1–7.
- McCormac FG, Hogg AG, Blackwell PG, Buck CE, Higham TFG, Reimer PJ. 2004. SHCAL04 Southern Hemisphere calibration, 0–11.0 cal. kyr BP. *Radiocarbon* 46(3):1087–92.
- Miramont C, Sivan O, Rosique T, Edouard JL, Jorda M. 2000. Subfossil tree deposits in the middle Durance (southern Alps, France); environmental changes from Allerod to Atlantic. *Radiocarbon* 42(3):423–35.

- Miramont C, Sivan O. 2008. Subfossil trees in the southern Alps of France, markers of the history of river landscapes. *Lettre pigb-pmrc France 21 - Changement global*. p 58–66.
- Miramont C, Sivan O, Guibal F, Kromer B, Talamo S, Kaiser KF. 2011. L'étalonnage du temps du radiocarbon par les cernes d'arbre. L'apport des series dendrochronologiques du gisement de bois sub-fossiles du torrent des Barbières (Alpes Françaises du sud). *Quaternaire* 22(3):261–71.
- Muscheler R, Kromer B, Björck S, Svensson A, Friedrich M, Kaiser KF, Southon J. 2008. Tree rings and ice cores reveal ^{14}C calibration uncertainties during the Younger Dryas. *Nature Geoscience* 1:263–7.
- Němec M, Wacker L, Hajdas I, Gäggeler H. 2010. Alternative methods for cellulose preparation for AMS measurement. *Radiocarbon* 52(2–3):1358–70.
- Passariello I, Marzaioli F, Lubritto C, Rubino M, D'Onofrio A, De Cesare N, Borriello G, Casa G, Palmieri A, Rogalla D, Sabbaresse C, Terrasi F. 2007. Radiocarbon sample preparation at the CIRCE AMS Laboratory in Caserta (Italy). *Radiocarbon* 49(2):225–32.
- Reimer PJ, Brown TA, Reimer RW. 2004. Discussion: reporting and calibration of post-bomb ^{14}C data. *Radiocarbon* 46(3):1299–1304.
- Reimer PJ, Bard E, Bayliss A, Beck JW, Blackwell PG, Bronk Ramsey C, Buck CE, Cheng H, Edwards RL, Friedrich M, Grootes PM, Guilderson TP, Hafidason H, Hajdas I, Hatté C, Heaton TJ, Hoffmann DL, Hogg AG, Hughen KA, Kaiser KF, Kromer B, Manning SW, Niu M, Reimer RW, Richards DA, Scott EM, Southon JR, Staff RA, Turney CSM, van der Plicht J. 2013. IntCal13 and Marine13 radiocarbon age calibration curves 0–50,000 years cal BP. *Radiocarbon* 55(4):1869–87.
- Rinne KT, Boettger T, Loader NJ, Robertson I, Switsur VR, Waterhouse JS. 2005. On the purification of α -cellulose from resinous wood for stable isotope (H, C and O) analysis. *Chemical Geology* 222:75–82.
- Rozanski K, Stichler W, Gonfiantini R, Scott EM, Beukens RP, Kromer B, van der Plicht J. 1992. The IAEA ^{14}C Intercomparison Exercise 1990. *Radiocarbon* 34(3):506–19.
- Santos GM, Bird MI, Fifield LK, Alloway BV, Chappell J, Hausladen PA, Arneith A. 2001. Radiocarbon dating of wood using different pretreatment procedures: application to the chronology of Rotoehu Ash, New Zealand. *Radiocarbon* 43(2A):239–48.
- Santos GM, Ormsby K. 2013. Behavioral variability in ABA chemical pretreatment close to the ^{14}C age limit. *Radiocarbon* 55(2–3):534–44.
- Schaub M, Kaiser KF, Frank DC, Buentgen U, Kromer B, Talamo S. 2008. Environmental change during the Allerød and Younger Dryas reconstructed from tree-ring data. *Boreas* 37:74–86.
- Scott EM, Cook GT, Naysmith P. 2010. The Fifth International Radiocarbon Intercomparison (VIRI): an assessment of laboratory performance in stage 3. *Radiocarbon* 52(2–3):859–65.
- Scott EM, Naysmith P, Cook GT. 2016. Interim report on SIRI with preliminary consensus values – June 2016. Unpublished.
- Sivan O, Miramont C, Édouard JL. 2006. Rythmes de la sédimentation et interprétations paléoclimatiques lors du Postglaciaire (Alpes du Sud) ^{14}C et dendro-géomorphologie, deux chronomètres complémentaires. *L'Érosion entre Société, Climat et Paléoenvironnement, Table ronde en l'honneur du Professeur René NEBOIT-GUILHOT Clermont-Ferrand*. p 423–8.
- Southon JR, Magana AL. 2010. A comparison of cellulose extraction and ABA pretreatment methods for AMS ^{14}C dating of ancient wood. *Radiocarbon* 52(2–3):1371–9.
- Staff RA, Reynard L, Brock F, Bronk Ramsey C. 2014. Wood pretreatment protocols and measurement of tree-ring standards at the Oxford Radiocarbon Accelerator Unit (ORAU). *Radiocarbon* 56(2):709–15.
- Stuiver M, Braziunas T. 1993. Sun, ocean, climate and atmospheric $^{14}\text{CO}_2$: an evaluation of causal and spectral relationships. *Holocene* 3:289–305.
- Stuiver M, Braziunas T. 1998. Anthropogenic and solar component of hemispheric ^{14}C . *Geophysical Research Letters* 25(3):329–32.
- Stuiver M, Polach HA. 1977. Discussion: reporting of ^{14}C data. *Radiocarbon* 19(3):355–63.
- Stuiver M, Quay PD. 1981. Atmospheric C changes resulting from fossil fuel CO_2 release and cosmic ray flux variability. *Earth and Planetary Science Letters* 53:349–62.
- Szymczak S, Joachimski MM, Bräuning A, Hetzer T, Kuhlemann J. 2011. Comparison of whole wood and cellulose carbon and oxygen isotope series from *Pinus nigra* ssp. *laricio* (Corsica/France). *Dendrochronologia* 29:219–26.
- Tans PP, De Jong AFM, Mook WG. 1978. Chemical pretreatment and radial flow of ^{14}C in tree rings. *Nature* 271:234–5.
- van der Plicht J, Hogg A. 2006. A note on reporting radiocarbon. *Quaternary Geochronology* 1:237–40.
- Vertregt N, de Vries FWTP. 1987. A rapid method for determining the efficiency of synthesis of plant biomass. *Journal of Theoretical Biology* 128(1):109–19.
- Wallis AFA, Wearne RH, Wright PJ. 1997. New approaches to the rapid analysis of cellulose in wood. *Proceedings of ISWPC: 9th International Symposium on Wood and Pulping Chemistry*. Montréal. C3:1–4.